Shahid Bahonar University of Kerman

Biomechanism and Bioenergy Research

Online ISSN: 2821-1855
Homepage: https://bbr.uk.ac.ir

Iranian Society of Agricultural Machinery Engineering and Mechanization

Intelligent-Oriented Virtual Prototyping of a 6-DOF Robotic Manipulator through Coupled Multibody Dynamics and Modal Analysis for Smart Agricultural Applications

Mohammad Mohammadi[1], Yousef Bazargan Lari[1]✉, Dara Fazel[1], Seyed Mohammad Reza Nazemosadat[1]

[1] Department of Mechanical Engineering, Shi.C., Islamic Azad University, Shiraz, Iran

✉ Corresponding author: yo.bazargan@iau.ac.ir

ARTICLE INFO

Article type:

Research Article

Article history:

Received 09 May 2026

Received in revised form 21 July 2026

Accepted 11 August 2026

Available Online 30 September 2026

Keywords:

Multibody Dynamics, 6-DOF Manipulator, Modal Analysis, Virtual Prototyping, Smart Agriculture, Contact Modeling

ABSTRACT

This study introduces a virtual prototyping framework that couples multibody dynamics with finite-element-based modal analysis to design and numerically assess a six-degree-of-freedom robotic manipulator for smart agricultural applications. A CAD model was developed in SolidWorks and imported into ADAMS to evaluate joint torques, accelerations, and compliant contact interactions under realistic motion cycles. Nonlinear damping and Coulomb friction were included to emulate soft-object grasping and placement. Simulations indicated sub-millimeter positioning accuracy (<0.5 mm), a peak base-joint torque of 15 N•m, and maximum transient accelerations of 3.2 m/s². Modal analysis of critical components identified natural frequencies ranging from 638 to 5856 Hz and maximum operational displacements ≤0.42 mm, providing a basis for assessing the system's vibrational and structural behavior. The unified multibody–modal loop addresses a gap in the literature by integrating contact-rich dynamics with structural verification, providing a simulation-based pathway for early-stage design that reduces reliance on costly physical prototypes. The framework also establishes a foundation for incorporating intelligent control, adaptive algorithms, and sensor-driven feedback in next-generation robotic manipulators for smart agriculture and precision automation.

Cite this article: Mohammadi, M., Bazargan Lari, Y., Fazel, D., & Nazemosadat, S. M. R (2026). Intelligent-Oriented Virtual Prototyping of a 6-DOF Robotic Manipulator through Coupled Multibody Dynamics and Modal Analysis for Smart Agricultural Applications. *Biomechanism and Bioenergy Research*, *5*(3), 1-17. https://doi.org/10.22103/bbr.2026.27632.1163

Publisher: Shahid Bahonar University of Kerman
DOI: https://doi.org/10.22103/bbr.2026.27632.1163

INTRODUCTION

Robotic manipulators are widely used in transportation, assembly, and industrial production because of their speed, precision, and ability to perform hazardous or repetitive tasks (Cruz et al., 2021; Nguyen-Tuong & Peters, 2011). Their design nevertheless requires accurate estimation of joint forces, torques, and motion-induced loads because these quantities directly influence performance, structural safety, and service life (Boyer & Porez, 2015; Z. Liu et al., 2023). Dynamic modeling and virtual prototyping allow potential problems related to stability, positioning, and mechanical response to be identified before physical construction, thereby reducing development time and cost (Boyer & Porez, 2015; Cruz et al., 2021). Agricultural robotics further requires manipulators to combine mechanical precision with adaptability to variable operating conditions, while broader smart-farming systems increasingly integrate robotic, AI-driven, and sustainable-energy technologies (Mohammadi, Nazemosadat, et al., 2026). (Li et al., 2024) developed a CNN–MLP-based configurable robotic arm for harvesting and crop inspection, while (P. H. Kuo et al., 2024) investigated intelligent optimization for control-error compensation and task scheduling. (Elgohr et al., 2025) also demonstrated the effectiveness of optimization-based path planning for collision-free robotic motion. More broadly, recent metaheuristic frameworks for constrained engineering design have demonstrated the potential of systematic search strategies for complex design-space exploration, providing a possible basis for future optimization of robotic design and control parameters (Mohammadi, Bazargan Lari, et al., 2026). These studies highlight the growing role of intelligent control and optimization, whereas the present work focuses on the mechanics-driven virtual-prototyping stage that precedes their future integration.

Dynamic and structural analyses are equally important for evaluating the mechanical reliability of robotic manipulators. (Pietruś & Gierlak, 2023) developed a two-link robot model and mapped resonance frequencies across configurations, with experiments confirming the simulations showing that arm posture strongly shapes low-frequency vibration (Mohammadi, Lari, et al., 2026). Building on this idea, we move beyond configuration-level analysis by coupling contact-rich multibody dynamics (ADAMS) with component-level finite-element modal verification in a single virtual-prototyping loop for a 6-DOF manipulator, targeting sub-millimeter precision in unstructured tasks. (Zhong et al., 2023) presented the design and simulation of a seven-degree-of-freedom hydraulic robotic arm using 7075 aluminum alloy, evaluating its strength through multibody dynamics and FEM-based structural analysis.

Recent independent studies further demonstrate the importance of considering manipulator dynamics, structural vibration, and contact behavior in agricultural robotics. (S. Liu et al., 2023) applied multibody dynamics together with experimental testing to investigate the kinematic characteristics of a robotic arm for mango harvesting. (Badkoobehhezaveh et al., 2022) combined finite-element and experimental modal analyses to characterize the vibration behavior of a long-reach robotic manipulator for farm applications, while (Alshihabi et al., 2025) integrated kinematic and dynamic analysis with FEA, modal analysis, and topology optimization to improve robotic-arm reliability and vibration performance. From the end-effector perspective, (Xie et al., 2024) explicitly considered contact behavior in the design of adaptive grippers for fruit-picking robots. Collectively, these independent studies highlight the complementary importance of motion, vibration, and contact-aware analysis and support the development of an integrated virtual-prototyping workflow for precision agricultural manipulation.

Similarly, (Dumitru et al., 2024) conducted a comprehensive dynamic study of a poly-articulated robot using MSC ADAMS and ANSYS, providing detailed kinematic and dynamic models to optimize motion and control.

However, most works do not combine dynamic simulation with modal structural analysis in a unified framework particularly for precision-oriented agricultural applications. To address this gap, the present study integrates both approaches within an integrated simulation architecture that serves as a virtual autonomous environment for robotic mechanism development. Multibody and CAD-based simulation tools have been widely used to predict robotic motion, joint loading, and potential design limitations before physical construction (Baglioni et al., 2016; Bahani et al., 2023; Pratheep et al., 2021; Wang et al., 2024). Complementary kinematic and trajectory-planning studies have further shown that accurate motion planning can reduce mechanical loading, energy demand, and task time (Y. L. Kuo & Huang, 2017; Lv et al., 2020; Mateo Sanguino & Andújar Márquez, 2012).

Previous studies have generally emphasized individual aspects of robotic system development. (Li et al., 2024) focused on intelligent agricultural manipulation, (Pietruś & Gierlak, 2023) examined configuration-dependent vibration behavior, (Zhong et al., 2023) combined multibody and structural analyses for a hydraulic manipulator, and (Dumitru et al., 2024) investigated detailed dynamic modeling of a poly-articulated robot. In contrast, the present study combines contact-rich multibody simulation of a complete pick-and-place cycle with component-level modal and displacement assessment within a single virtual-prototyping workflow specifically directed toward delicate agricultural object handling. The novelty therefore lies not in the individual use of ADAMS or FEM, but in their coordinated application to simultaneously evaluate motion, actuator loading, compliant contact behavior, positioning performance, and structural response of a 6-DOF agricultural manipulator. This framework is intended as an early-stage computational design and assessment tool, while physical-prototype testing remains necessary for subsequent experimental validation.

MATERIALS AND METHODS

Design and Simulation of the Robotic Arm

The six-degree-of-freedom robotic arm analyzed in this study was designed using SolidWorks software and transferred to the ADAMS environment for detailed dynamic simulation and performance evaluation. This process aimed to assess the arm's behavior in handling delicate agricultural packages, focusing on joint forces, torques, motion profiles, and contact stability under realistic working conditions. During the design phase, carbon steel was selected for all arm components. With a density of 7801 kg/m^3, Young’s modulus of 2.07×10^{11} N/m^2, and a Poisson’s ratio of 0.29, it was chosen for its robust mechanical properties, ensuring adequate strength and load-bearing capability suitable for repetitive handling of lightweight yet fragile produce.

After completion of the 3D CAD model, the robotic arm was imported into ADAMS, where the revolute joints, motor drivers, and contact interfaces required for the six-degree-of-freedom mechanism were defined. Each joint was driven by a prescribed step-sequence actuator input. The motion cycle consisted of two main stages: (1) approach and lifting of the object and (2) controlled transfer and placement on the target platform. The actuator inputs are reported in (Table 1), while (Figure 2) illustrates four representative configurations of the prescribed pick-and-place trajectory. Contact interactions were defined between the grippers and the manipulated object and between the object and the supporting platforms. A compliant contact formulation was employed with a stiffness of 1×10^{8} N/m, a damping coefficient of 1×10^{4}, a penetration depth of 1×10^{-4} m, and a force exponent of 2.2. Static and dynamic Coulomb friction coefficients of 0.3 and 0.1, respectively, were applied. (Figure 3) shows the resulting multibody model, including the actuators, contact interfaces, and environmental boundaries.

Figure 1. Structure of a Six-Degree-of-Freedom Robotic Arm with Rotational Constraints.

Table 1. Step Sequence for Reciprocal Movements of Robotic Arm Motors.

Motor	Step Sequence (Backward Movement)	Step Sequence (Forward Movement)
Base Rotation	Step (time, 1.1, 0, 2, 88.5d)	Step (time, 0, 0, 1, -56d)
Shoulder Rotation	Step (time, 1.1, 0, 2, -25d)	Step (time, 0, 0, 1, 104d)
Elbow Rotation	Step (time, 1.1, 0, 2, -50d)	Step (time, 0, 0, 1, 90d)
Wrist Rolling	–	Step (time, 0, 0, 1, 10d)
Upper Arm	Step (time, 1.1, 0, 2, -10d)	Step (time, 0, 0, 1, 4d)
Gripper Rotation	–	Step (time, 0, 0, 1, 0d)

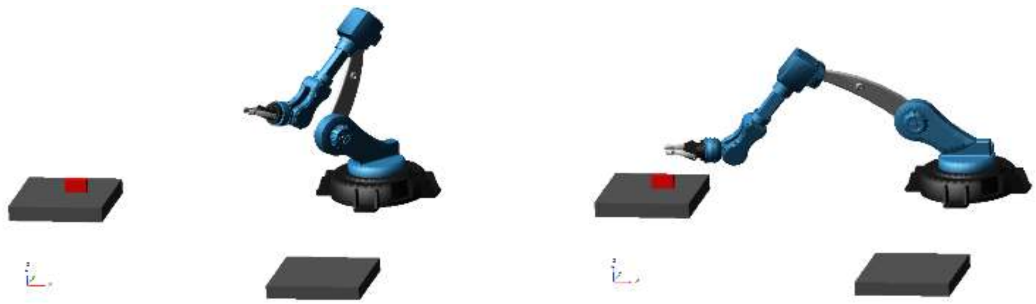

(a) Initial Position (b) Above Grasping Position

(c) Grasping Position (d) Releasing Position

Figure 2. Simulation of the Robotic Arm's Motion Path in Four Positions.

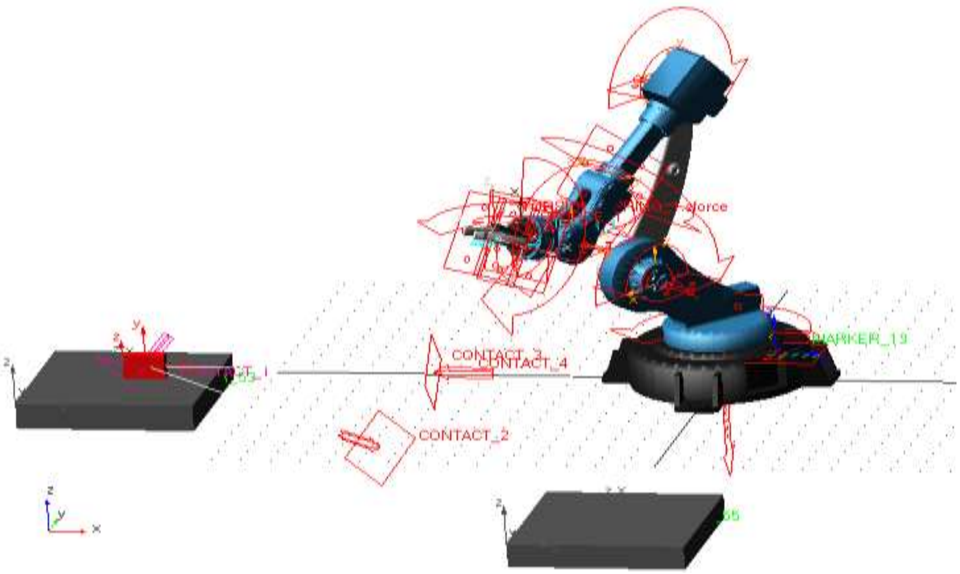

Figure 3. Simulated Model of the Robotic Arm with Contact Constraints.

A torsional spring enhanced the gripper's precision during object acquisition and release. Positioned between the two segments of the gripper, the spring was configured with a stiffness of 50 N·m/deg and a damping coefficient of 5 N·m·s/deg, delivering sufficient torque to ensure secure handling of the object. Additionally, a preloaded torque of -200 N·m was applied to enhance responsiveness and repeatability during precision grasping operations. Gravitational acceleration ($g = 9.81$ m/s^2) was used in the negative Z-axis direction to simulate realistic environmental effects on the system. These configurations contributed to a physically consistent simulation environment replicating agricultural packaging and transfer scenarios.

The dynamic simulation was executed in ADAMS/View using the built-in simulation controller over a total duration of 3 s with 200 simulation steps. Initial-condition reset was disabled, and continuous graphical rendering was used to monitor the prescribed motion and contact transitions. The primary dynamic outputs evaluated during the simulation included linear and angular accelerations, joint torques, contact forces, and final positioning. The torsional spring and compliant contact formulations described above were retained throughout the complete motion cycle. These settings define the numerical conditions under which the dynamic results reported in (Figures 4–14) were obtained and provide the basis for the subsequent structural assessment.

Numerical Verification and Validation Scope

Because the present work focuses on early-stage virtual prototyping, a physical prototype and experimental dataset were not available for direct experimental validation. Accordingly, the computational model was evaluated through complementary numerical checks at different levels. These included successful execution of the prescribed pick-and-place motion cycle, continuous evaluation of joint forces, torques, accelerations, contact responses, and final positioning during the multibody simulation, together with FEM-based modal and displacement assessments of the critical structural components. These complementary analyses provide numerical verification of the model behavior across the kinematic, dynamic, contact, and structural domains; however, they should not be interpreted as a substitute for experimental validation. Therefore, the quantitative results reported in this study represent model-based predictions under the stated assumptions, and subsequent prototype and field testing will be required to establish experimental agreement.

RESULTS AND DISCUSSION

Simulation Results and System Performance Evaluation

This section presents a detailed evaluation and interpretation of the simulation results to assess the dynamic behavior and mechanical performance of the six-degree-of-freedom robotic arm, tailored explicitly for precision agricultural product handling. Both numerical and graphical data including linear and angular accelerations, applied torques, contact forces, and joint responses were examined to assess actuator effectiveness, mechanical coordination, motion stability, and overall design feasibility.

The linear acceleration profile (Figure 4) demonstrated peak values of 3.2 m/s², particularly during the initial lifting and transition phases. These rapid increases in acceleration reflect the system's ability to respond swiftly to positional changes, which is essential in high-speed agricultural tasks such as fruit sorting. However, the initial overshoot could be optimized using advanced control strategies like adaptive or AI-based controllers. The minimum acceleration (0.8 m/s²) observed during the settling phase suggests efficient damping and energy dissipation through mechanical constraints and actuator tuning.

Angular velocities (Figure 5), peaking at 2.5 rad/s, remained consistent with minimal fluctuation, indicating precise control without excessive oscillations. Compared to the work by (Li et al., 2024), which employed neural-based motion planning for flexible arm movement, this system achieved similar precision without requiring learning-based feedback, relying instead on well-defined trajectory inputs. Contact forces recorded at 120 N and 95 N (Figures 6 and 7) were maintained within safe thresholds, confirming the gripper's mechanical integrity and the softness of interactions with objects and platforms. In contrast with (Zhong et al., 2023), where hydraulic actuation modulated force during high-load manipulation, this electromechanical system achieved stable contact using only structural tuning and impact-damping parameters. The torque requirement of Motor 1 (Figure 8) peaked at 15 N·m, aligning well with the theoretical design constraints. This motor is the base actuator and sustains the bulk of the initial inertial response.

Any excess load or oscillation at this joint would risk destabilizing the whole kinematic chain. Fortunately, no such instability was observed during the simulation. Likewise, linear forces across axes (Figure 9), peaking at 180 N on the x-axis, reflected balanced load distribution, indicating a well-proportioned mechanical design. Angular acceleration (Figure 10) reached 1.8 rad/s², with final angular velocities (Figure 11) stabilizing at 2.0 rad/s. The final positioning error (Figure 13), which remained below 0.5 mm, demonstrates the system's capacity to perform repetitive positioning tasks accurately. The combined force/torque equilibrium (Figure 12) and overall system dynamics (Figure 14) confirmed synchronized performance without signs of overstrain, backlash, or erratic motion.

From a simulation-based design assessment perspective, these findings support the mechanical feasibility of the robotic arm within the modeled agricultural operation. Nevertheless, the results should be interpreted as numerical predictions rather than experimental validation. The current simulation environment does not include real-world disturbances such as external wind, unexpected contact shifts, or sensor noise, and real-time feedback-based adjustments are not implemented. These limitations may influence the system response during actual deployment. Future work should therefore include prototype-based measurements and field trials to quantitatively compare simulated and measured motion, load, contact, and structural responses. Within the present scope, the results provide a computational basis for further design refinement and subsequent physical implementation.

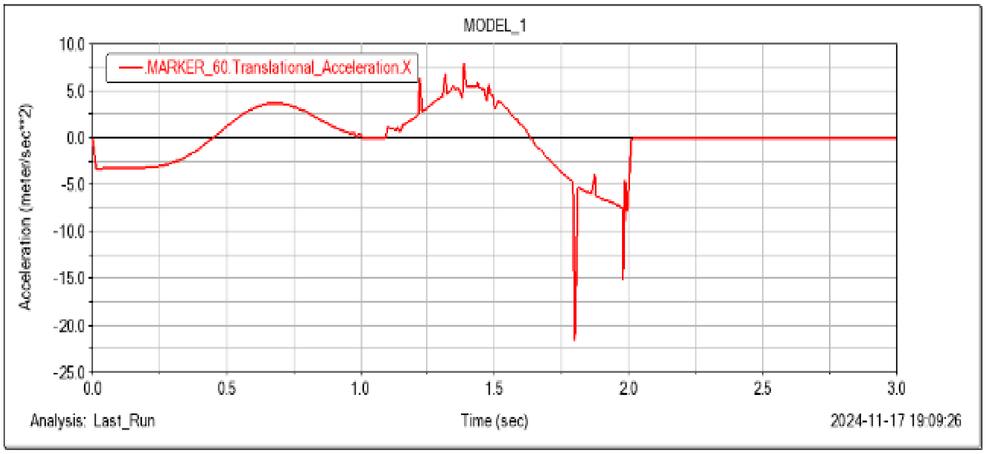

Figure 4. Linear acceleration of the robotic arm during different motion phases.

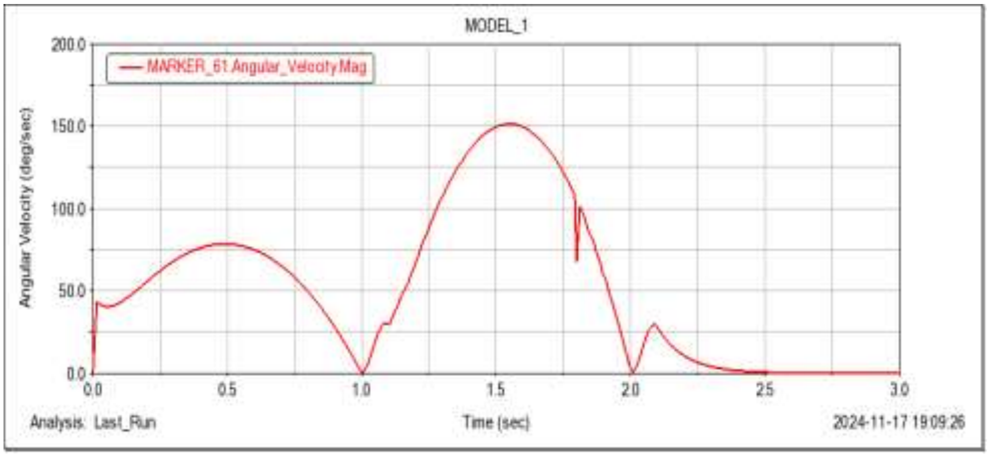

Figure 5. Angular velocity of the robotic arm's joints.

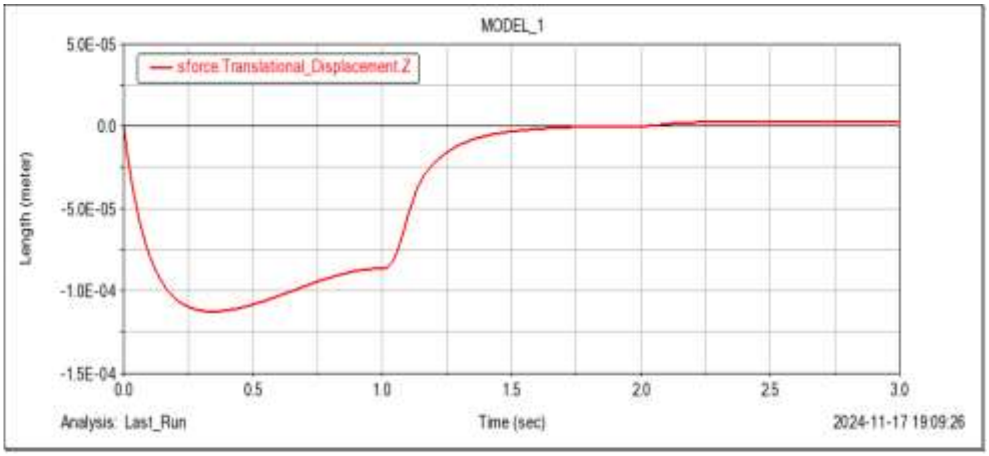

Figure 6. Initial contact forces (Contact 1) between the grippers and the box.

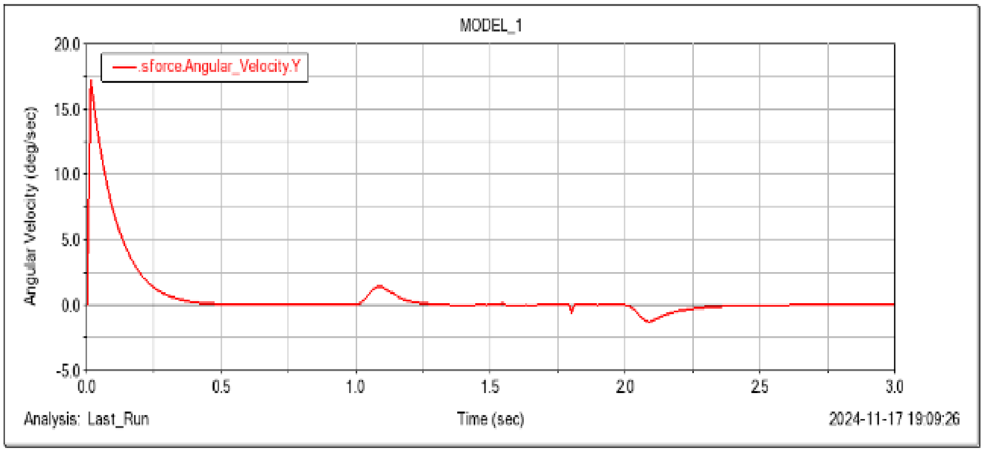

Figure 7. Contact forces at the second platform (Contact 4).

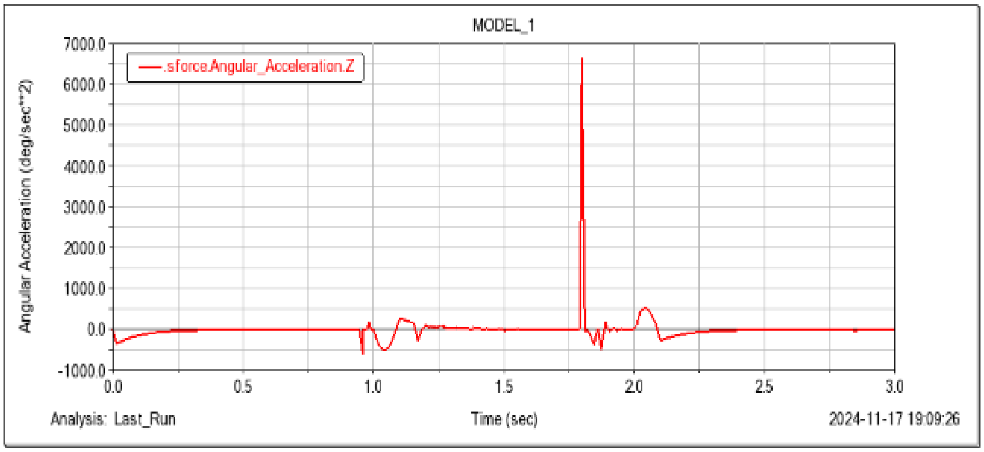

Figure 8. Torque applied by Motor 1.

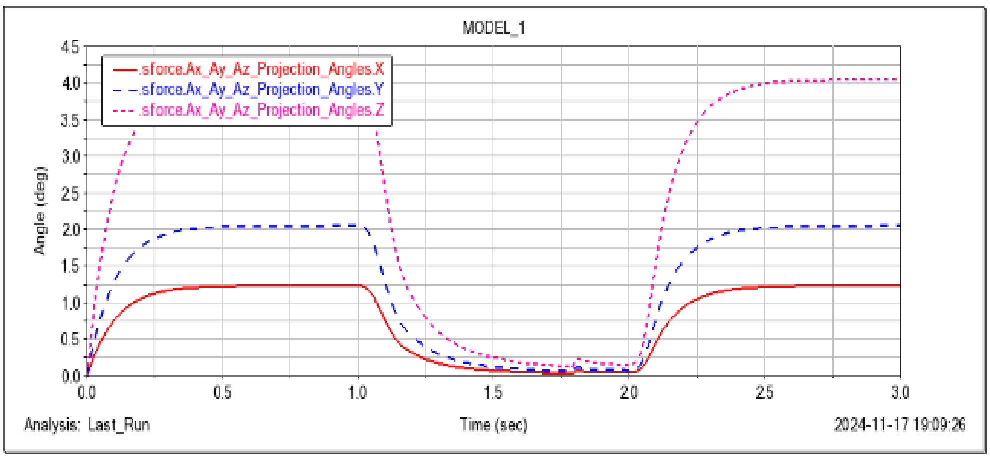

Figure 9. Linear forces of the robotic arm across various axes.

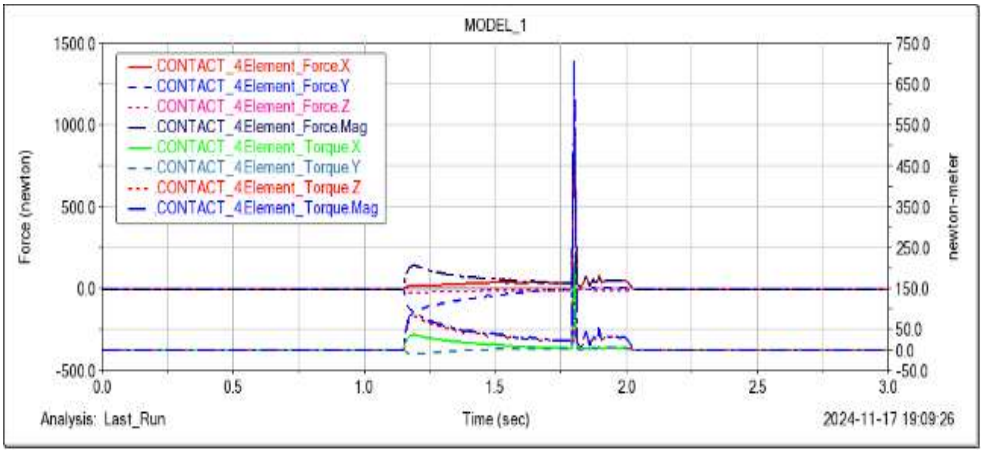

Figure 10. Angular acceleration of the robotic arm's joints.

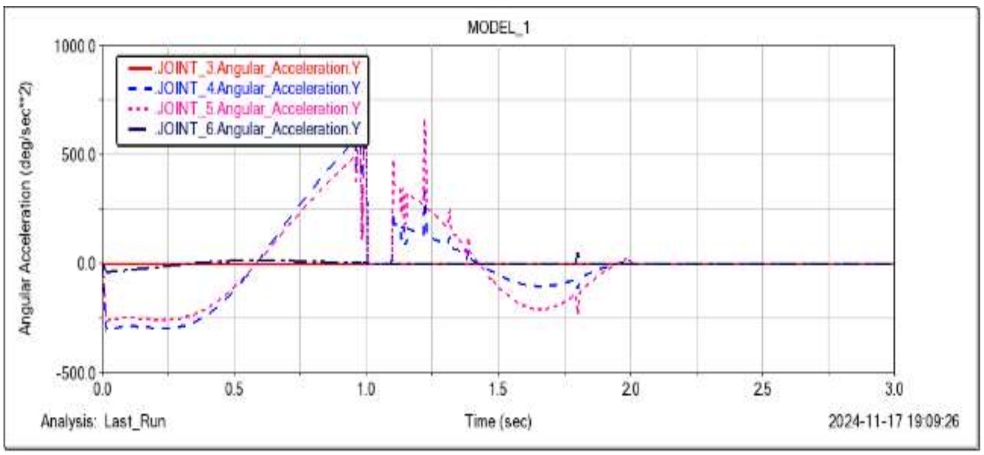

Figure 11. Final angular velocity of the robotic arm.

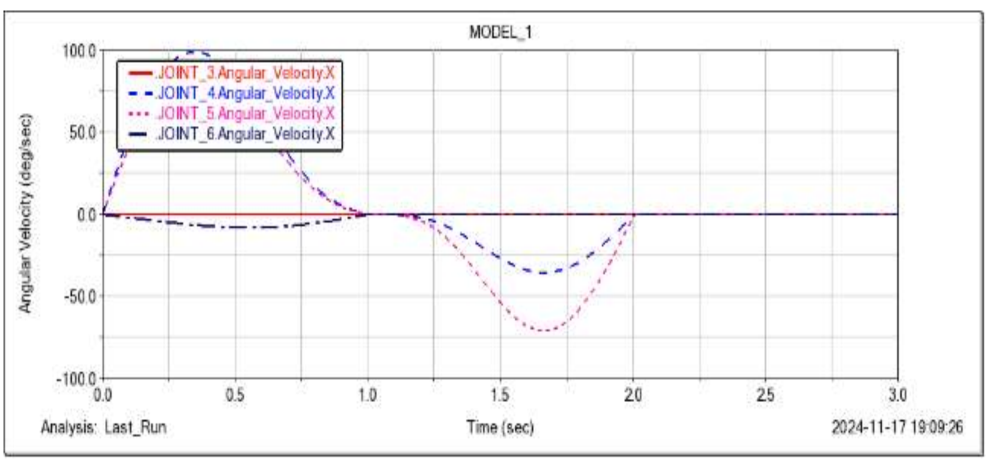

Figure 12. Combined forces and torques during motion.

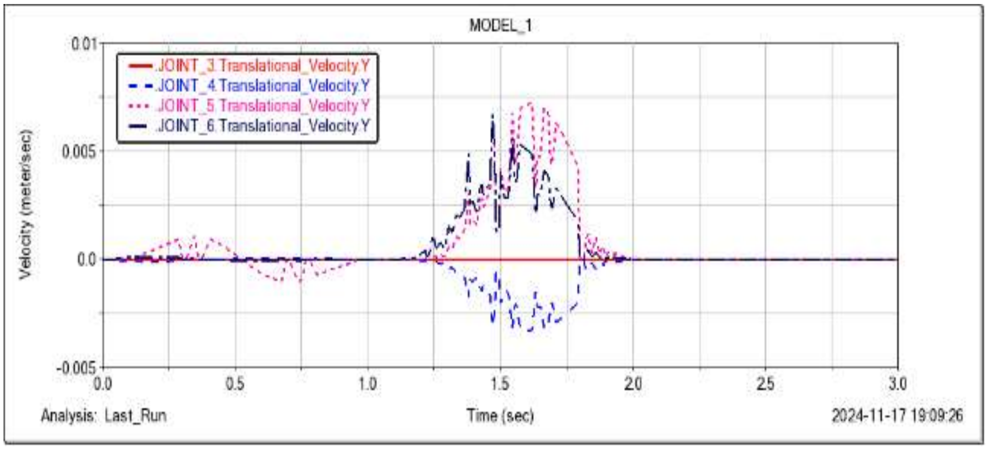

Figure 13. The final position of the robotic arm.

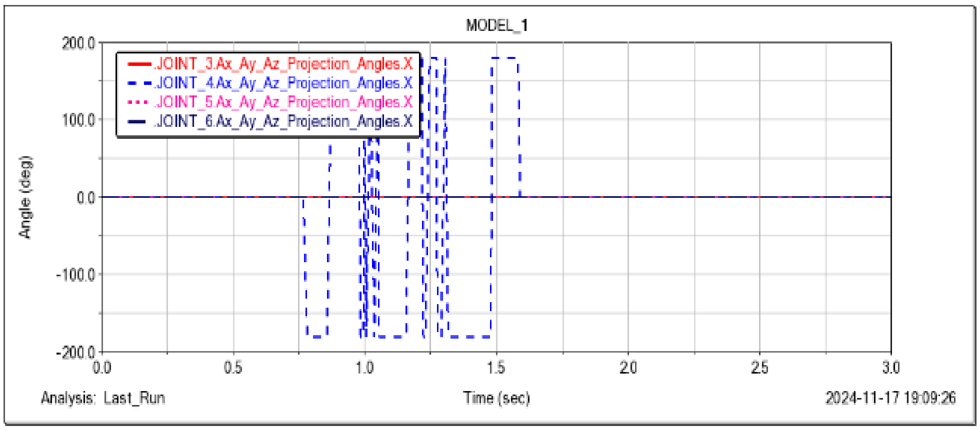

Figure 14. Overall system force diagram during simulation.

Structural Modal and Displacement Analysis of Robotic Arm Components Using Finite Element Method

To complement the multibody dynamic analysis, component-level FEM-based modal and displacement assessments were performed for the base rotation segment, shoulder joint, and wrist rolling section. These components were selected because of their important load-bearing and motion-transmission roles during the complete manipulation cycle. The first five natural vibration modes of each component, including bending and torsional modes, were extracted using the FEM capabilities within the ADAMS/View workflow. Linear tetrahedral elements were used for discretization, and the corresponding node and element counts are reported in (Table 3). FEM-based static and dynamic investigations of mechanically loaded engineering structures have similarly demonstrated the usefulness of modal response and displacement fields for identifying structurally critical regions and supporting subsequent design refinement (Mohammadi et al., 2024; Nazemosadat et al., 2025). The modal analysis was used to characterize the natural frequencies and associated mode shapes, whereas the displacement analysis was used to assess deformation under the modeled operational loading condition. Independent robotic-arm studies support the use of modal analysis as an early-stage structural assessment tool. (Badkoobehhezaveh et al., 2022) combined finite-element analysis with experimental modal analysis for a farm manipulator, while (Alshihabi et al., 2025) incorporated modal analysis and topology optimization to improve vibration behavior and structural reliability. These studies support modal characterization as a useful basis for identifying vibration-sensitive components and guiding subsequent structural refinement.

Related multiphysics investigations have also shown that integrating FEM-based modal assessment with complementary simulation domains can reveal structural and performance limitations that may remain less evident in single-domain analyses (Mohammadi et al., 2025). Additionally, a displacement contour under operational loading conditions was generated. The results of this analysis (Figure 18) show that the overall deformation of the system is minimal, with maximum displacement not exceeding 0.42 mm. This low level of deformation supports the structural adequacy of the design under the modeled working loads, an essential factor for maintaining precision in the handling of agricultural products. The combination of modal and displacement analyses indicates favorable structural stability within the modeled conditions and, through the identification of low-frequency modes, provides a suitable basis for future vibration and damping optimization. These results support the expected structural suitability of the robotic arm for sensitive and repetitive agricultural applications under the modeled conditions.

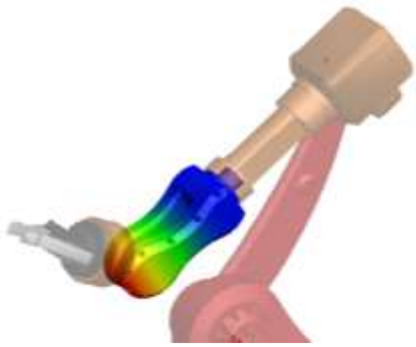

(a) Mode 1 – Bending, 1050.96 Hz

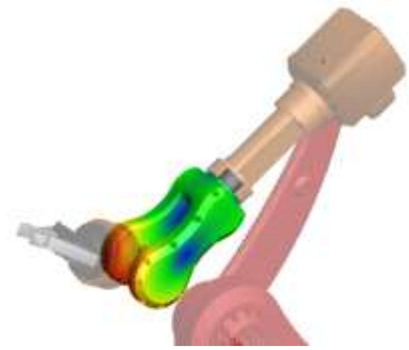

(b) Mode 2 – Torsional, 1934.20 Hz

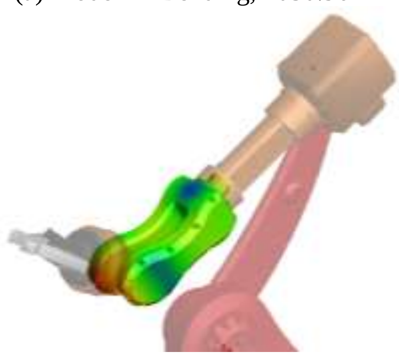

(c) Mode 3 – Coupled Bending–Torsional, 2918.39 Hz

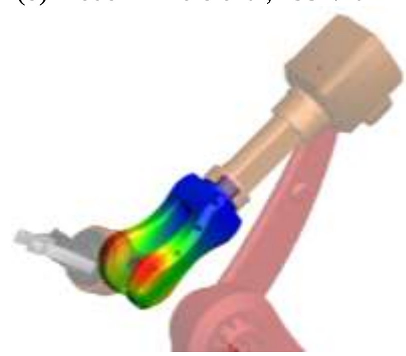

(d) Mode 4 – Higher-Order Bending, 3805.80 Hz

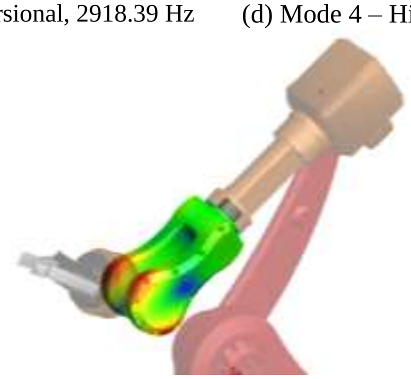

(e) Mode 5 – Higher-Order Torsional, 4726.27 Hz

Figure 15. First five vibration mode shapes of the wrist component; the corresponding mode type and natural frequency are indicated in each subfigure.

Table 2. Natural frequencies (Hz) of the first five vibration modes for each robotic arm component.

Component	Mode 1 (Hz)	Mode 2 (Hz)	Mode 3 (Hz)	Mode 4 (Hz)	Mode 5 (Hz)
Wrist	١٠٥٠,٩٦	١٩٣٤,٢٠	٢٩١٨,٣٩	٣٨٠٥,٨٠	٤٧٢٦,٢٧
Shoulder	٦٣٨,١٥	١١٨١,٧٨	١٦٥٤,٢٣	١٨٤٨,٦٧	٣٣٥٩,٤٦
Base	١٦٦١,٨٩	٢٤٠٢,٩٧	٣١٥٥,٣٩	٤٣١٣,٥٣	٥٨٥٦,٧٩

Because the prescribed ADAMS STEP commands are transient rather than periodic, they do not define a single exact excitation frequency. Therefore, a characteristic operational excitation frequency was estimated from the inverse of the transition time, $f_{char} \approx 1/\Delta t$. For the forward commands, $\Delta t = 1.0\ s$, corresponding to approximately $1.00\ Hz$, whereas the return commands have $\Delta t = 0.9\ s$, corresponding to approximately $1.11\ Hz$. The lowest calculated natural frequency is $638.15\ Hz$; therefore, even relative to the highest characteristic step-motion frequency, the frequency-separation ratio is approximately 574. This substantial separation indicates that direct resonance with the primary step-motion timescale is unlikely under the modeled operating sequence. A detailed spectral assessment of transient load harmonics would require a dedicated FFT-based analysis and is therefore reserved for future investigation.

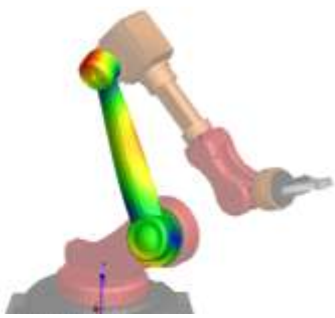

(a) Mode 1 – Bending, 638.15 Hz

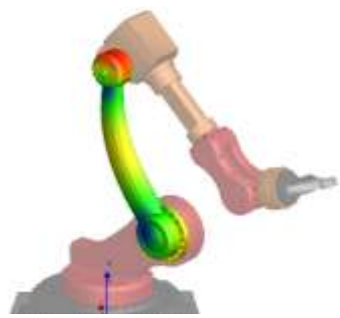

(b) Mode 2 – Torsional, 1181.78 Hz

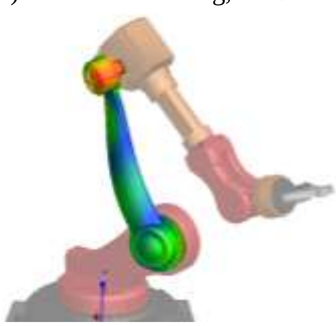

(c) Mode 3 – Coupled Bending–Torsional, 1654.23 Hz

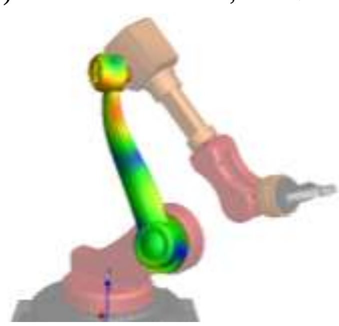

(d) Mode 4 – Higher-Order Bending, 1848.67 Hz

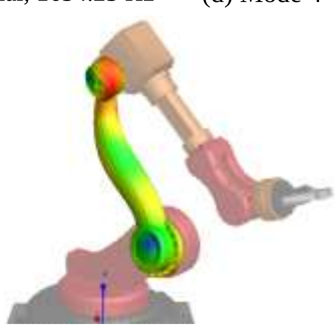

(e) Mode 5 – Higher-Order Torsional, 3359.46 Hz

Figure 16. First five vibration mode shapes of the shoulder component; the corresponding mode type and natural frequency are indicated in each subfigure.

Table 3. Mesh specifications of robotic arm components (using linear tetrahedral elements).

Component	Element Type	Nodes	Elements
Base	Linear Tetrahedral	4237	17609
Shoulder	Linear Tetrahedral	2262	8243
Wrist	Linear Tetrahedral	2857	10474

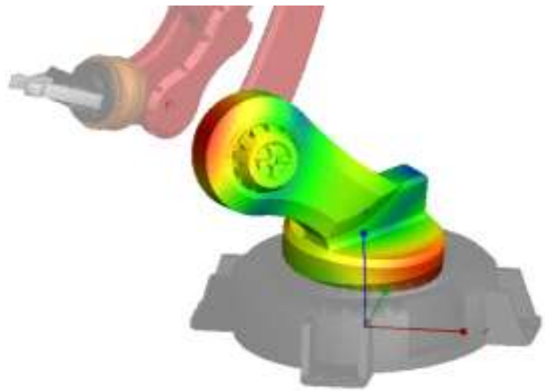

(a) Mode 1 – Bending, 1661.89 Hz

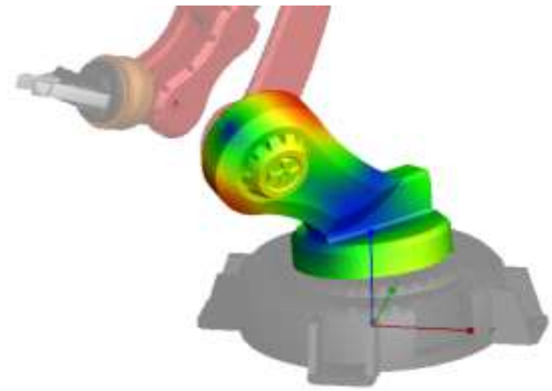

(b) Mode 2 – Torsional, 2402.97 Hz

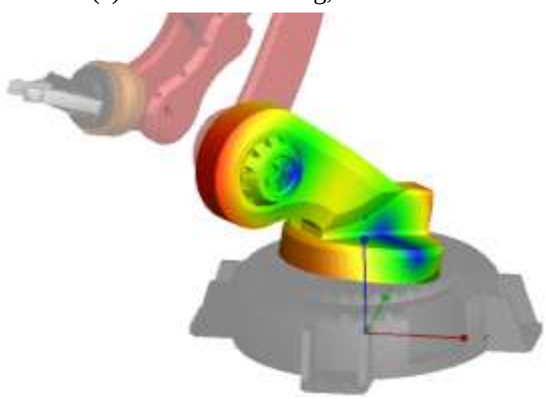

(c) Mode 3 – Coupled Bending–Torsional, 3155.39 Hz

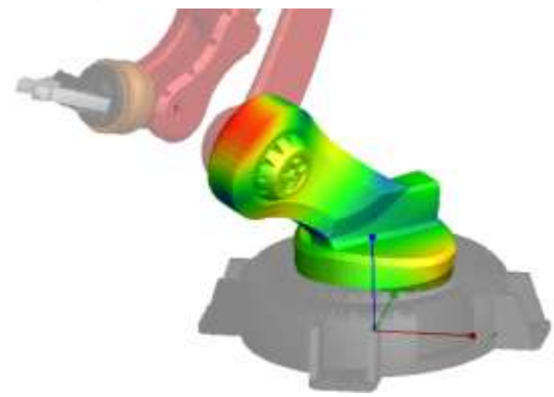

(d) Mode 4 – Higher-Order Bending, 4313.53 Hz

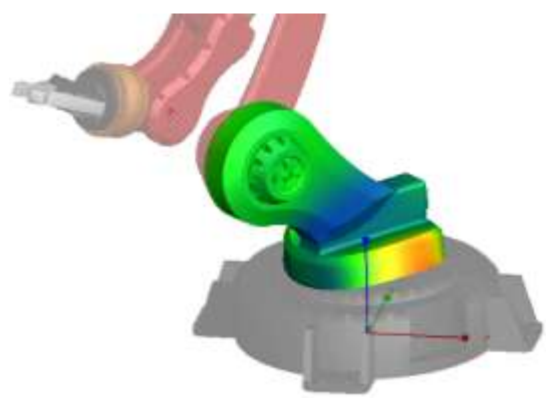

(e) Mode 5 – Higher-Order Torsional, 5856.79 Hz

Figure 17. First five vibration mode shapes of the base rotation component; the corresponding mode type and natural frequency are indicated in each subfigure.

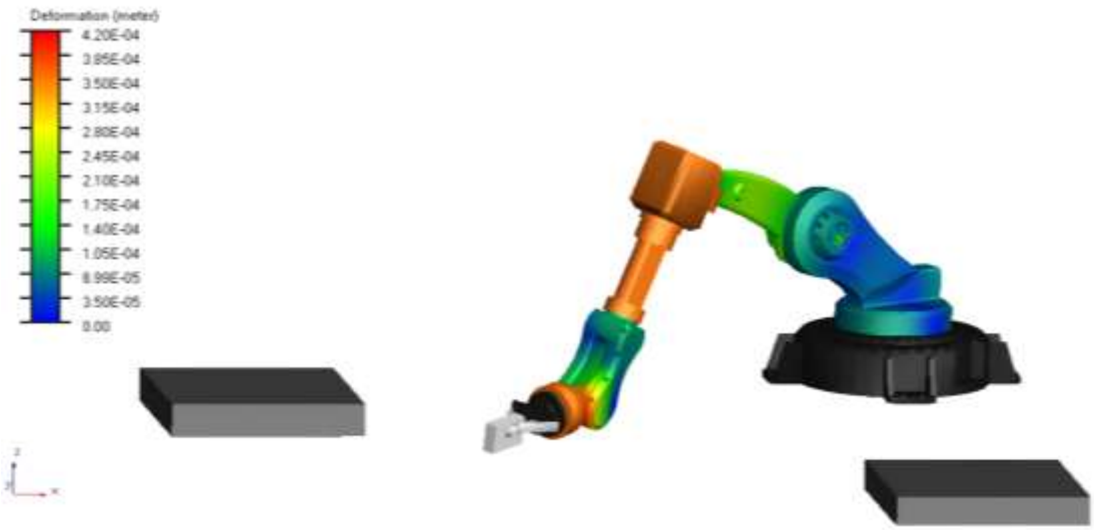

Figure 18. Displacement contour of the complete robotic arm under the modeled operational loading condition; the color scale represents total deformation in meters.

Comparative Evaluation of Applied Simulation Methods

To enhance the clarity of the methodology and findings presented in this study, a comparative table (Table 4) has been included to summarize the characteristics, numerical outcomes, advantages, and limitations of the primary simulation methods employed. This table emphasizes the significance of integrating dynamic analysis with structural evaluation and provides a comprehensive understanding of the system's mechanical performance in agricultural applications.

Table 4. Comparative summary of this study's simulation and analysis methods, including quantitative results, advantages, and known limitations.

Method / Tool	**Type of Analysis**	**Key Numerical Results**	**Advantages**	**Limitations**
ADAMS (Dynamic Simulation)	Multibody dynamic analysis of motion, torques, accelerations	- Max linear acceleration: (3.2 m/s²) - Max torque: (15 N·m) - Positioning accuracy: (<0.5 mm)	High-fidelity motion modeling, actuator and constraint interaction, precise trajectory simulation	It does not account for structural deformation and no fatigue/stress analysis.
FEM (Modal & Displacement Analysis)	Modal analysis, static displacement evaluation	- Max displacement: (0.42 mm) - Natural frequencies: 638–5856 Hz; characteristic STEP-motion frequency: 1.00–1.11 Hz	Identifies deformation and modal behavior; large separation from the characteristic step-motion frequency	No time-based actuation response lacks real-time dynamics.
Integrated ADAMS + FEM	Hybrid dynamic-structural framework	- Complementary assessment across motion and structural domains - Large frequency separation, low displacement	Combines motion-level and structural analyses within a unified virtual-prototyping workflow.	No physical-prototype or experimental validation; environmental variability is excluded.

CONCLUSION

This study presents a simulation-based virtual-prototyping framework that links contact-rich multibody dynamics with component-level modal and displacement assessment for a 6-DOF manipulator intended for precision agricultural handling. Rather than treating motion performance and structural behavior as separate design problems, the proposed workflow enables actuator loading, contact interaction, positioning behavior, and vibration-sensitive structural response to be considered within a common computational framework before physical prototyping.

The broader scientific implication of this approach is that precision manipulation of delicate agricultural products depends not only on kinematic performance but also on the interaction between transient loading, contact mechanics, and structural dynamics. Coupling these domains at the design stage provides a more physically informed basis for identifying critical joints and components, evaluating design trade-offs, and prioritizing structural or control modifications. Although developed for an agricultural manipulation scenario, the workflow can also be extended to other robotic systems in which contact sensitivity, positioning performance, and structural vibration must be assessed simultaneously.

The present study remains computational and should therefore be interpreted within the assumptions of the multibody and finite-element models. Physical-prototype validation, environmental disturbances, sensor uncertainty, material variability, and closed-loop feedback were not included in the present framework. These limitations establish a clear path for subsequent experimental and control-oriented development.

Future work should prioritize prototype-based dynamic and modal measurements, field trials under realistic agricultural conditions, sensitivity and uncertainty analyses of contact and material parameters, and the integration of vision, tactile sensing, and adaptive control. Extending the framework toward fatigue, stress, and detailed excitation-spectrum (FFT) analyses would further support the development of robust manipulators for smart agriculture and other high-precision automation tasks.

FUNDING SOURCES

This research received no external funding.

DATA AVAILABILITY STATEMENT

No data was used for the research described in the article.

DECLARATION OF COMPETING INTEREST

The authors declare no conflict of interest.

REFERENCES

Alshihabi, M., Ozkahraman, M., & Kayacan, M. Y. (2025). Enhancing the reliability of a robotic arm through lightweighting and vibration control with modal analysis and topology optimization. *Mechanics Based Design of Structures and Machines*, *53*(3), 1950–1974. https://doi.org/10.1080/15397734.2024.2400207

Badkoobehhezaveh, H., Fotouhi, R., Zhang, Q., & Bitner, D. (2022). Vibration Analysis of a 5-DOF Long-Reach Robotic Arm. *Vibration 2022, Vol. 5, Pages 585-602*, *5*(3), 585–602. https://doi.org/10.3390/VIBRATION5030034

Baglioni, S., Cianetti, F., Braccesi, C., & De Micheli, D. M. (2016). Multibody modelling of N DOF robot arm assigned to milling manufacturing. Dynamic analysis and position errors evaluation. *Journal of Mechanical Science and Technology 2016 30:1*, *30*(1), 405–420. https://doi.org/10.1007/S12206-015-1245-0

Bahani, A., El houssine Ech-Chhibat, M., Samri, H., & Elattar, H. A. (2023). The Inverse Kinematics Evaluation of 6-DOF Robots in Cooperative Tasks Using Virtual Modeling Design and Artificial Intelligence Tools. *International Journal of Mechanical Engineering and Robotics Research*, *12*(2), 121–130. https://doi.org/10.18178/IJMERR.12.2.121-130

Boyer, F., & Porez, M. (2015). Multibody system dynamics for bio-inspired locomotion: from geometric structures to computational aspects. *Bioinspiration & Biomimetics*, *10*(2), 025007. https://doi.org/10.1088/1748-3190/10/2/025007

Cruz, G. L., Alazki, H., Cortes-Vega, D., & Rullán-Lara, J. L. (2021). Application of Robust Discontinuous Control Algorithm for a 5-DOF Industrial Robotic Manipulator in real-time. *Journal of Intelligent & Robotic Systems 2021 101:4*, *101*(4), 75-. https://doi.org/10.1007/S10846-020-01282-1

Dumitru, S., Copilusi, C., Dumitru, N., & Geonea, I. (2024). A Dynamic Analysis of a Poly-Articulated Robot. *Computation 2024, Vol. 12, Page 156*, *12*(8), 156. https://doi.org/10.3390/COMPUTATION12080156

Elgohr, A. T., Kasem, H. M., & Elhadidy, M. S. (2025). Comparative analysis of robotic arms path planning techniques: case study of the KUKA KR4 R600 using the Whale optimization algorithm. *International Journal of Intelligent Robotics and Applications 2025 10:1*, *10*(1), 209–226. https://doi.org/10.1007/S41315-025-00501-Y

Kuo, P. H., Syu, M. J., Yin, S. Y., Liu, H. H., Zeng, C. Y., Lin, W. C., & Yau, H. T. (2024). Intelligent optimization algorithms for control error compensation and task scheduling for a robotic arm. *International Journal of Intelligent Robotics and Applications 2024 8:2*, *8*(2), 334–356. https://doi.org/10.1007/S41315-024-00328-Z

Kuo, Y. L., & Huang, P. Y. (2017). Experimental and simulation studies of motion control of a Delta robot using a model-based approach. *International Journal of Advanced Robotic Systems*, *14*(6). https://doi.org/10.1177/1729881417738738

Li, M., Wu, F., Wang, F., Zou, T., Li, M., & Xiao, X. (2024). CNN-MLP-Based Configurable Robotic Arm for Smart Agriculture. *Agriculture 2024, Vol. 14, Page 1624*, *14*(9), 1624. https://doi.org/10.3390/AGRICULTURE14091624

Liu, S., Wang, F., Lin, M., Liu, J., & Yao, K. (2023). Analysis and test of the kinematics characteristics of the robotic arm for a mango harvesting vehicle. *Transactions of the Chinese Society of Agricultural Engineering*, *40*(1), 58–67. https://doi.org/10.11975/J.ISSN.1002-6819.202306172

Liu, Z., Peng, K., Han, L., & Guan, S. (2023). Modeling and Control of Robotic Manipulators Based on Artificial Neural Networks: A Review. *Iranian Journal of Science and Technology - Transactions of Mechanical Engineering*, *47*(4), 1307–1347. https://doi.org/10.1007/S40997-023-00596-3

Lv, Y., Peng, Z., Qu, C., & Zhu, D. (2020). An adaptive trajectory planning algorithm for robotic belt grinding of blade leading and trailing edges based on material removal profile model. *Robotics and Computer-Integrated Manufacturing*, *66*, 101987. https://doi.org/10.1016/J.RCIM.2020.101987

Mateo Sanguino, T. J., & Andújar Márquez, J. M. (2012). Simulation tool for teaching and learning 3D kinematics workspaces of serial robotic arms with up to 5-DOF. *Computer Applications in Engineering Education*, *20*(4), 750–761. https://doi.org/10.1002/CAE.20433

Mohammadi, M., Bazargan Lari, Y., & Bazargan Lari, K. (2026). Centipede optimization algorithm: Best-of-L local search with contractive consensus for constrained engineering optimization. *Neurocomputing*, *659*, 131774. https://doi.org/10.1016/J.NEUCOM.2025.131774

Mohammadi, M., Lari, Y. B., & Nazemosadat, S. M. R. (2026). Vibration-based non-destructive evaluation of dual cracks in bidirectionally functionally graded nanobeams: a nonlocal elasticity–metaheuristic optimisation framework for structural health monitoring. *Nondestructive Testing and Evaluation*. https://doi.org/10.1080/10589759.2026.2713683

Mohammadi, M., Nazemosadat, S. M. R., & Afsari, A. (2024). Modeling and Analysis of a Tractor Diesel Engine Test Stand Structure Using the Finite Element Method. *Biomechanism and Bioenergy Research*, *3*(2), 75–87. https://doi.org/10.22103/BBR.2024.24161.1090

Mohammadi, M., Nazemosadat, S. M. R., Bazargan Lari, Y., Afsari, A., & Bahramkia, A. (2026). A Review of Solar-Powered, Robotic, and AI-Driven Agricultural Machinery for Smart and Sustainable Farming. *Biomechanism and Bioenergy Research*, *5*(1), 41–61. https://doi.org/10.22103/BBR.2026.26353.1141

Mohammadi, M., Nazemosadat, S. M. R., Fazel, D., & Bazargan Lari, Y. (2025). An integrated approach for structural modeling, modal analysis, and aerodynamic evaluation of an electric vehicle body shell using finite element method and computational fluid dynamics. *Materials Today Communications*, *45*, 112331. https://doi.org/10.1016/J.MTCOMM.2025.112331

Mohammadi, M., Nazemosadat, S. M. R., & Afsari, A. (2025). Advanced Modeling and Analysis of Diesel Engine Test Support Structure (ETSS) Using (FEM) and (XFEM): A Comprehensive Study on Fracture Mechanics, Fatigue Life, and Modal Analysis of Crack Growth. *International Journal of Advanced Design and Manufacturing Technology, Issue 3, Vol. 18, p. 25-42*. https://doi.org/10.71644/admt.2025.1198975

Nguyen-Tuong, D., & Peters, J. (2011). Model learning for robot control: a survey. *Cognitive Processing 2011 12:4*, *12*(4), 319–340. https://doi.org/10.1007/S10339-011-0404-1

Pietruś, P., & Gierlak, P. (2023). Influence of the Manipulator Configuration on Vibration Effects. *Acta Mechanica et Automatica*, *17*(4), 515–522. https://doi.org/10.2478/AMA-2023-0060

Pratheep, V. G., Chinnathambi, M., Priyanka, E. B., Ponmurugan, P., & Thiagarajan, P. (2021). Design and Analysis of six DOF Robotic Manipulator. *IOP Conference Series: Materials Science and Engineering*, *1055*(1), 012005. https://doi.org/10.1088/1757-899X/1055/1/012005

Wang, X., Xuan, H., Zhao, S., Ye, K., & Dai, L. (2024). Co-simulation Research of Pipeline Welding Robot Based on MATLAB and ADAMS. *Proceedings - 2024 International Conference on Intelligent Computing and Robotics, ICICR 2024*, 162–168. https://doi.org/10.1109/ICICR61203.2024.00038

Xie, B., Jin, M., Duan, J., Li, Z., Wang, W., Qu, M., & Yang, Z. (2024). Design of Adaptive Grippers for Fruit-Picking Robots Considering Contact Behavior. *Agriculture (Switzerland)*, *14*(7), 1082. https://doi.org/10.3390/AGRICULTURE14071082/S1

Zhong, J., Jiang, W., Zhang, Q., & Zhang, W. (2023). Design and Simulation of a Seven-Degree-of-Freedom Hydraulic Robot Arm. *Actuators 2023, Vol. 12, Page 362*, *12*(9), 362. https://doi.org/10.3390/ACT12090362